



## Optimization of and mechanism for the coagulation–flocculation of oil-field wastewater from polymer flooding

Qunbiao He<sup>a</sup>, Chen Deng<sup>a</sup>, Ying Xu<sup>a</sup>, Danni Shen<sup>b,c</sup>, Bin Dong<sup>a,b,\*</sup>, Xiaohu Dai<sup>a,\*</sup>

<sup>a</sup>The State Key Laboratory of Pollution Control and Resource Reuse, Tongji University, Shanghai 200092, P.R. China, Tel. +86 21 6598 1372; email: 418652271@qq.com (Q. He), Tel. +86 183 0195 3610; email: dengchen01@126.com (C. Deng), Tel. +86 188 1758 1865; email: tjfogy@sina.com (Y. Xu), Tel. +86 21 6598 1794; emails: tj\_dongbin@163.com (B. Dong), hawk101eagle@163.com (X. Dai)

<sup>b</sup>Ningbo Institute of Technology, Zhejiang University, Ningbo 315100, P.R. China, Tel. +86 159 0378 1639; email: 15903781639@126.com (D. Shen)

<sup>c</sup>School of Environmental and Chemical Engineering, Dalian Jiao Tong University, Dalian 116021, P.R. China

Received 2 July 2015; Accepted 26 December 2015

### ABSTRACT

Oil-field wastewater from polymer flooding (OWPF) is difficult to deal with because it contains a high concentration of partially hydrolyzed polyacrylamide (HPAM), which stabilizes the wastewater. Coagulation–flocculation with polyepichlorohydrin–dimethylamine (EPI-DMA) and polymeric aluminum ferric chloride (PAFC) was used to optimize the treatment of OWPF. HPAM and COD removal were optimized using the response surface method (RSM), based on the Box–Behnken design (BBD). The variables EPI-DMA dose, PAFC dose, and pH were selected as the factors in the RSM to investigate their individual and interaction effects on the response values, HPAM and COD removal efficiencies. The results showed that HPAM and COD removal efficiencies of 95.4 and 85.7%, respectively, could be reached using 0.65 mg/L EPI-DMA, 924 mg/L PAFC, and pH 5.51. Fourier transform infrared spectroscopy, zeta potential, particle size analysis, scanning electron microscopy, and energy dispersive spectroscopy were used to study the mechanism of the coagulation–flocculation process. The results indicated that the main functions of the EPI-DMA and PAFC in the coagulation–flocculation process were electric neutralization, adsorption, and sweeping.

**Keywords:** Oil-field wastewater from polymer flooding (OWPF); Response surface method (RSM); Coagulation–flocculation process; HPAM removal; Polyepichlorohydrin–dimethylamine (EPI-DMA)

### 1. Introduction

China produced  $2.1 \times 10^8$  tons of petroleum in 2014. The enhanced oil recovery process of polymer flooding is playing an increasingly significant role in oil production. A great deal of wastewater containing

high concentrations of polymer is therefore being produced [1,2]. However, oil-field wastewater from polymer flooding (OWPF) is difficult to deal with due to the presence of complex components, especially partially hydrolyzed polyacrylamide (HPAM) [3,4]. A high concentration of HPAM in OWPF can give rise to

\*Corresponding authors.

a high oil content, turbidity, and high chemical oxygen demand, which overload the existing treatment process [5].

In a wastewater system, HPAM combines with metal ions to produce a curled up molecular chain [6,7]. The charged carboxylate radical ( $-\text{COO}^-$ ) on the HPAM molecular chain dissociates in solution, resulting in a negatively charged surface. This increases the charge potential of the particles' surfaces and the electrostatic repulsion between the particles. The solvation of the  $-\text{COO}^-$  groups causes a hydration shell around the negatively charged particles, greatly enhancing the stability of the system (Fig. 1). The existing wastewater treatment process cannot treat this HPAM-enriched wastewater effectively. The HPAM in OWPF does not fully degrade. It therefore accumulates in the environment, causing environmental pollution and potential threats [8]. HPAM removal during OWPF treatment is thus crucial.

Researchers have recently put forward different opinions as to whether the HPAM in OWPF is biodegradable [9–12]. An efficient, economical OWPF treatment process is urgently needed. Coagulation–flocculation is a simple, effective way of treating sewage and has become a common technology used in various wastewater treatment processes [13–15]. Coagulation–flocculation has recently been used to deal with OWPF. Existing studies have tested a series of coagulants and flocculants, attaining different oil removal rates and turbidities [4,16–18]. However, HPAM, the most critical pollutant in this wastewater, has not drawn sufficient research attention.

The treatment efficiency of coagulation–flocculation is determined by a variety of factors [19–23] and can be significantly improved by the proper optimization of these factors. The response surface method (RSM) has been successfully used to optimize coagulation

and describe the effects of individual factors and their interactions [24–26].

In our previous studies, a combination of polyepichlorohydrin–dimethylamine (EPI-DMA) and polymeric aluminum ferric chloride (PAFC) was chosen as the coagulant–flocculant for treating OWPF by coagulation–flocculation. The effect of pH was also studied. The major aim of this study was to treat OWPF with coagulation–flocculation and optimize this treatment using an RSM approach. The efficiencies of HPAM and COD removal were selected as the response value and the optimal levels of three factors, EPI-DMA dose, PAFC dose, and pH, were obtained. Fourier transform infrared (FTIR) spectrophotometry, size distributions, zeta potential, scanning electron microscopy (SEM), and energy dispersive spectroscopy (EDS) were used to interpret the mechanism by which coagulation–flocculation works. The effective treatment method optimized with the RSM developed in this study may provide a theoretical basis for the treatment of OWPF.

## 2. Materials and methods

### 2.1. Materials

The OWPF sample was collected from the settling tank of an oily wastewater treatment plant in Daqing, China. Indicators describing the wastewater sample and the variation range of the OWPF are shown in Table 1. These indicators were obtained using the standard method for determining the quality of water and wastewater. The HPAM concentrations were measured using starch–cadmium iodine [27].

### 2.2. Experimental operation

Jar tests were used to carry out the coagulation–flocculation experiments, using 500-mL beakers with 400 mL of wastewater and a magnetic stirrer. The influence of different values of the three variables—pH (5, 6, 7), EPI-DMA dose (0.4, 0.6, 0.8 mg/L), and PAFC dose (500, 750, 1,000 mg/L)—were investigated. The dosages were determined by the single-factor tests in the previous studies. The scheme of the coagulation–flocculation process is shown in Fig. 2. The pH of the OWPF was adjusted with 0.1 mol/L  $\text{H}_2\text{SO}_4$  solution under rapid mixing. EPI-DMA was then added to the wastewater with 200 rpm stirring for 3 min. Finally, PAFC was added to the wastewater with rapid stirring at 200 rpm for 3 min. Once all three were added, the solution was slowly stirred at 50 rpm for 15 min. The solution was left to settle for 30 min, then the supernatant 2 cm below the water surface was removed. The concentration of HPAM and COD

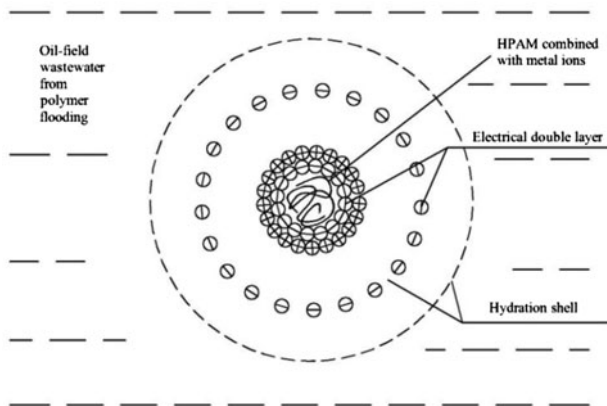


Fig. 1. Schematic view of HPAM stabilization in OWPF.

Table 1  
Characteristics of OWPF

Indicators	Oil (mg/L)	Iron (mg/L)	Alkalinity (mg/L)	Hardness (mg/L)	pH value	Viscosity (mPa s)
Wastewater sample	57.98 ± 4.31	2.20 ± 0.13	1,001 ± 66	121.1 ± 9.2	7.85 ± 0.04	1.70 ± 0.04
Variation range	30–70	–	800–1,100	90–140	7.5–9.0	–
Indicators	TDS (mg/L)	Sulphion (ug/L)	Chlorion (mg/L)	COD (mg/L)	Silicon (mg/L)	HPAM (mg/L)
Value	3,050 ± 178	719 ± 89	950 ± 46	880 ± 33	27.67 ± 4.47	595 ± 21
Variation range	2,500–3,500	–	800–1,150	500–900	–	300–600

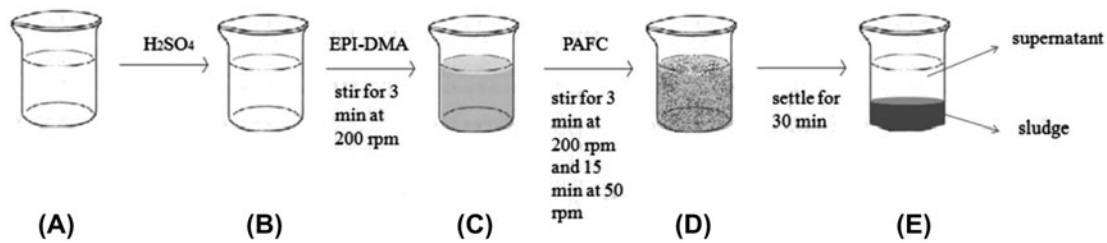


Fig. 2. Scheme for the coagulation–flocculation experiments.

were measured and removal efficiencies were calculated with Eq. (1):

$$R = \left(1 - \frac{C}{C_0}\right) \times 100\% \quad (1)$$

where  $R$  is the removal efficiency,  $C_0$  is the concentration in the wastewater (mg/L), and  $C$  is the concentration in the supernatant (mg/L).

### 2.3. Experimental design and data analysis

Design Expert software can perform experimental design, data analysis, and design optimization. In this study, all three functions were used in Design Expert 8.0.6. The Box–Behnken design (BBD) was used to carry out a response surface design. The BBD method is a response surface design method based on spherical space design. It optimizes the experimental condi-

tions using as few tests as possible [28]. The experimental design factors and level coding values are shown in Table 2.

HPAM and removal were selected as the response value. According to the regression analysis, a second-order model was fit to the experimental data to describe the relationship between the response value and factors:

$$Y_m = b_0 + \sum_{i=1}^k b_i X_i + \sum_{i=1}^k b_{ii} X_i^2 + \sum_{i < j} \sum_j b_{ij} X_i X_j \quad (2)$$

where  $Y_m$  is the predicted response value;  $b_0$ ,  $b_i$ ,  $b_{ii}$ , and  $b_{ij}$  are the offset term,  $i$ th linear coefficient, quadratic coefficient, and  $ij$ th interaction coefficient, respectively; and  $X_i$  and  $X_j$  are the values of each factor.

The experimental design provided by the software is presented in Table 3.

Table 2  
Box-Behnken experimental design factors and level coding values

Factor	Name	Unit	Low actual (-1)	High actual (1)	Central actual (0)
$X_1$	EPI-DMA dosage	mg/L	0.4	0.8	0.6
$X_2$	PAFC dosage	mg/L	500	1,000	750
$X_3$	pH value		5	7	6

Table 3  
BBD and response results for the study of three experimental variables

Run	Factor			Response	
	EPI-DMA dosage ( $X_1$ )	PAFC dosage ( $X_2$ )	pH value ( $X_3$ )	HPAM removal (%)	COD removal (%)
1	0	0	0	92.7	81.2
2	0	-1	-1	83.1	58.5
3	0	0	0	92.5	80.7
4	1	0	-1	89.1	83.0
5	0	1	-1	95.2	81.7
6	1	1	0	89.9	86.4
7	-1	0	1	76.4	55.9
8	1	0	1	89.9	82.6
9	-1	-1	0	74.5	52.3
10	0	0	0	93.0	81.1
11	0	0	0	92.1	81.7
12	-1	1	0	82.9	62.1
13	0	-1	1	83.4	61.4
14	-1	0	-1	84.4	54.7
15	0	0	0	92.3	81.0
16	1	-1	0	88.9	64.6
17	0	1	1	90.4	79.1

#### 2.4. FTIR spectra

The OWPF, OWPF-dosed EPI-DMA, sludge, and supernatant samples were freeze-dried to produce powder samples. The OWPF-dosed EPI-DMA sample was obtained after centrifugation for 5 min at 3,000 rpm to separate the particles from the solution (step C in Fig. 2). This centrifugation did not affect the results. One milligram of each sample was dispersed evenly in 150 mg of KBr and the mixtures were pelleted. These pellets were analyzed on a Thermo Fisher Nicolet 6700 FTIR spectrometer in the range 4,000–400  $\text{cm}^{-1}$ .

#### 2.5. Zeta potential and particle size

The zeta potential and particle size distribution of the particles in the OWPF with added EPI-DMA were measured using a Malvern Mastersizer ZS-90.

#### 2.6. SEM and EDS

SEM and EDS of the freeze-dried samples were performed using a Hitachi s-4800 equipped with an EDS. A dialyzed sample of the OWPF was prepared for the SEM and EDS analysis by freeze-drying.

Table 4  
ANOVA for HPAM removal

Source	Sum of squares	DF	Mean square	F-value	p-value ( $p > F$ )
Model	554.34	9	61.59	29.86	<0.0001
$X_1$	196.02	1	196.02	95.02	<0.0001
$X_2$	101.53	1	101.53	49.22	0.0002
$X_3$	17.11	1	17.11	8.29	0.0237
$X_1X_2$	13.69	1	13.69	6.64	0.0367
$X_1X_3$	19.36	1	19.36	9.38	0.0182
$X_2X_3$	6.5	1	6.5	3.15	0.1191
$X_1^2$	140.3	1	140.3	68.01	<0.0001
$X_2^2$	30.64	1	30.64	14.85	0.0063
$X_3^2$	13.6	1	13.6	6.59	0.0371
Residual error	14.44	7	2.06		
Lack of fit	13.95	3	4.65	38.12	0.0021
Pure error	0.49	4	0.12		
Total	568.78	16			

The other samples were prepared as for the FTIR spectra analysis.

### 3. Results and discussion

#### 3.1. Analysis of HPAM removal

The measured HPAM removal efficiencies achieved by coagulation–flocculation are shown in Table 3. The standard polynomial regression method was used to fit the experimental data. The following second-order model equation was obtained:

$$\begin{aligned}
 Y_1 = & 92.52 + 4.95 X_1 + 3.56 X_2 - 1.46 X_3 - 1.85 X_1 X_2 \\
 & + 2.20 X_1 X_3 - 1.28 X_2 X_3 - 5.77 X_1^2 - 2.70 X_2^2 \\
 & - 1.80 X_3^2
 \end{aligned}
 \tag{3}$$

Analysis of variance (ANOVA) is a widely used method for analyzing the relationships between variables and their influence, and for evaluating the significance of a model [29]. The HPAM removal efficiencies were subjected to ANOVA tests. The results are

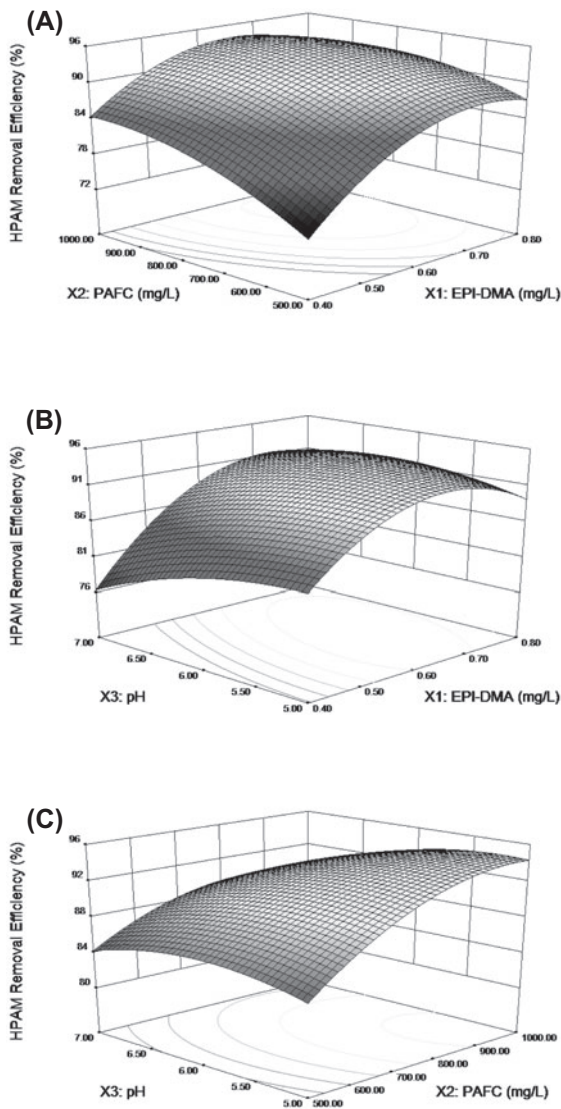


Fig. 3. Surface graphs of HPAM removal showing the effect of variables: (A) EPI-DMA dosage–PACF dosage (pH is 6.0), (B) EPI-DMA dosage–pH (PACF dosage is 750 mg/L), and (C) PACF dosage–pH (EPI-DMA dosage is 0.6 mg/L).

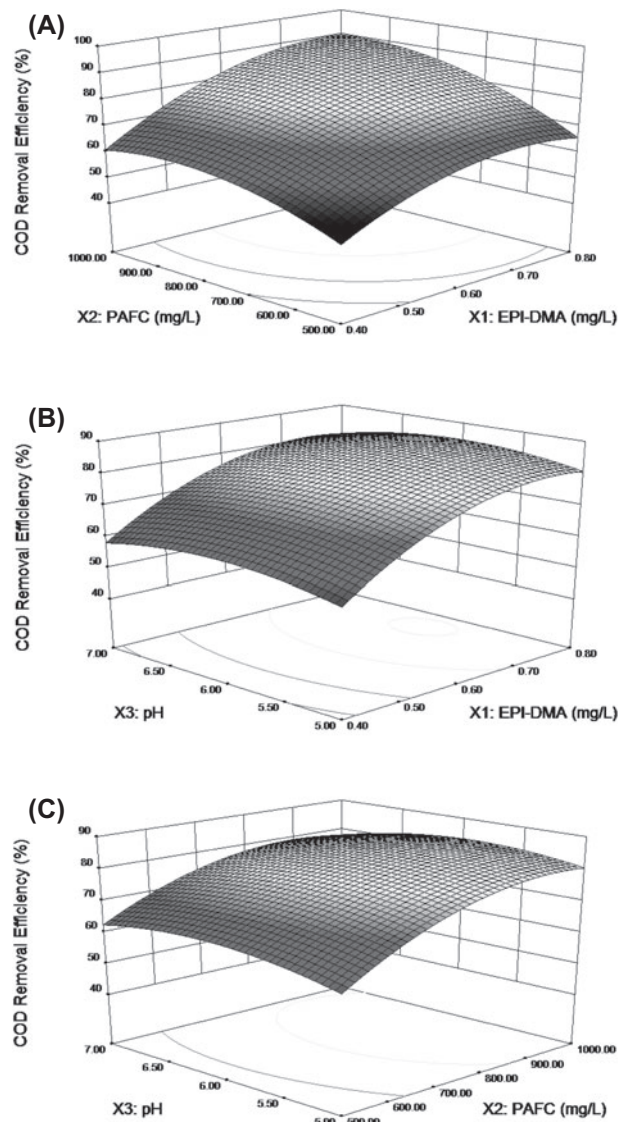


Fig. 4. Surface graphs of COD removal showing the effect of variables: (A) EPI-DMA dosage–PACF dosage (pH is 6.0), (B) EPI-DMA dosage–pH (PACF dosage is 750 mg/L), and (C) PACF dosage–pH (EPI-DMA dosage is 0.6 mg/L).

Table 5  
ANOVA for COD removal

Source	Sum of squares	DF	Mean square	F-value	p-value ( $p > F$ )
Model	2342.78	9	260.31	33.94	<0.0001
$X_1$	1,048.82	1	1,048.82	136.73	<0.0001
$X_2$	657.03	1	657.03	85.66	<0.0001
$X_3$	0.15	1	0.15	0.02	0.8923
$X_1X_2$	36.00	1	36.00	4.69	0.0670
$X_1X_3$	0.64	1	0.64	0.08	0.7811
$X_2X_3$	7.56	1	7.56	0.99	0.3538
$X_1^2$	266.62	1	266.62	34.76	0.0006
$X_2^2$	196.56	1	196.56	25.63	0.0015
$X_3^2$	71.91	1	71.91	9.37	0.0183
Residual error	53.69	7	7.67		
Lack of fit	53.16	3	17.72	133.24	0.0002
Pure error	0.53	4	0.13		
Total	2,396.48	16			

presented in Table 4. The F value is used to describe the significance of the interaction between each variable, also called the interactive relationship between the variables. The ANOVA results indicated that the second-order model was significant, according to Fisher's *F*-test ( $F = 29.86$ ). The *p*-value was very low ( $p < 0.0001$ ), indicating that there was only a 0.01% probability that the *F*-value was caused by noise in the system. The regression coefficient ( $R^2$ ) of the model was 0.9746, demonstrating that only 2.54% of the total variance could not be explained by the regression equation. Adequate precision usually requires a ratio of more

than 4. The ratio of the model was 18.734, indicating that the fitted model illustrated the design area. The variables and their interactions had different influences on HPAM removal.  $X_1$ ,  $X_2$ ,  $X_3$ ,  $X_1X_2$ ,  $X_1X_3$ ,  $X_1^2$ ,  $X_2^2$ , and  $X_3^2$  were significant terms ( $p < 0.05$ ) and  $X_1$ ,  $X_2$ ,  $X_1^2$ , and  $X_2^2$  were very significant terms ( $p < 0.01$ ). EPI-DMA dose, PAFC dose, pH, and the interaction effects of EPI-DMA with PAFC and EPI-DMA with pH were therefore the key factors in HPAM removal.

Following the regression equation, the response surfaces between the factors and response value were drawn, as shown in Fig. 3.

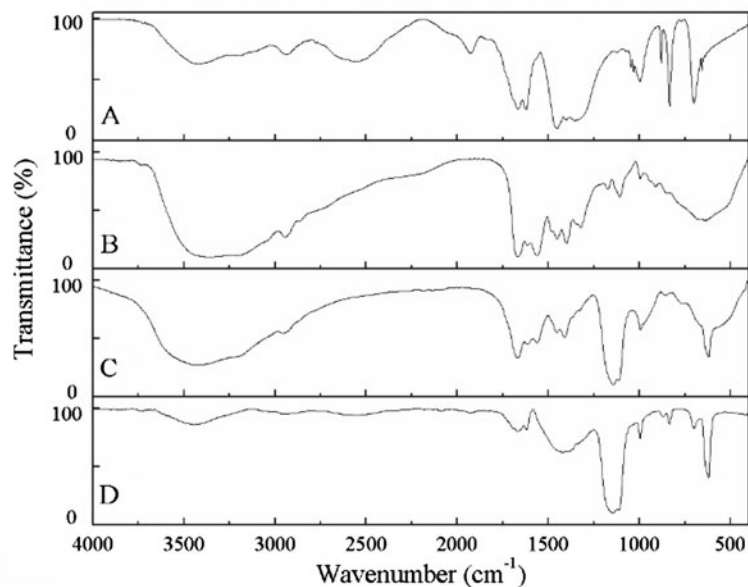


Fig. 5. FTIR spectral of freeze-drying samples of (A) OWPF, (B) OWPF-dosed EPI-DMA, (C) sludge, and (D) supernatant.

Fig. 3 clearly shows that HPAM removal gradually increased with an increase in EPI-DMA and PAFC and a decrease in pH. When the factors reached a certain value, the HPAM removal efficiency reached a maximum and then declined. As the EPI-DMA dose increased, the HPAM removal efficiency gradually increased, then decreased and changed significantly. The surface variation trend was steeper. The EPI-DMA dose therefore had a more pronounced effect on the HPAM removal. As the PAFC dose increased, the HPAM removal followed the same trend as with the EPI-DMA dose, but showed a slower change. The pH value had less effect than the other two factors. During coagulation, the change in pH value may have had a small effect on the EPI-DMA and PAFC, and may have also affected the state of the HPAM in the wastewater. The EPI-DMA dose may have played the largest role in the process because EPI-DMA has a higher positive charge density than traditional flocculants, so may have destroyed the hydrated shell of the HPAM more easily and neutralized the HPAM's negative charge [30,31]. Although the effect of the PAFC alone on HPAM removal was not obvious, PAFC had a significant effect, suggesting that adsorption and sweeping actions play an important role in this process.

### 3.2. Analysis of COD removal

The measured COD removal efficiencies achieved by coagulation–flocculation are shown in Table 3. The following equation was obtained by a regression model:

$$\begin{aligned}
 Y_2 = & 81.14 + 11.45 X_1 + 9.06 X_2 + 0.14 X_3 \\
 & + 3.00 X_1 X_2 - 0.40 X_1 X_3 - 1.38 X_2 X_3 - 7.96 X_1^2 \\
 & - 6.83 X_2^2 - 4.13 X_3^2
 \end{aligned}
 \quad (4)$$

The ANOVA results (Table 5) indicated that the model was significant since Fisher's  $F$ -test ( $F = 33.94$ ). The  $p$ -value ( $p < 0.0001$ ) also indicated that the  $F$  value caused by noise would occur with only a 0.01% probability. The regression coefficient ( $R^2$ ) of the model was 0.9776, demonstrating that only 2.24% of the total variance could not be explained by the regression equation. The adequate precision of the model was 19.313, indicating that the fitted model illustrated the design space. The variables and their interactions had different influences on COD removal.  $X_1$ ,  $X_2$ ,  $X_1^2$ ,  $X_2^2$ , and  $X_3^2$  were significant terms ( $p < 0.05$ ) and  $X_1$ ,  $X_2$ ,  $X_1^2$ , and  $X_2^2$  were very significant terms ( $p < 0.01$ ). EPI-DMA dose and PAFC dose were the key factors in

COD removal. And the response surfaces were shown in Fig. 4.

It can be found from the response surfaces (Figs. 3 and 4) that the removal of HPAM and COD had the similar tendency with the increase in dosage and the COD removal approached to a quite high level as the HPAM removal reached the maximum. It was indicated that HPAM was the main source which led to a high concentration of COD in the OWPF, although there were other pollutants in it such as oil droplets, humic acid, and microbial metabolism products. And a long-term monitoring also showed the phenomenon (Table 1). Therefore, HPAM removal was the key to COD removal of the OWPF.

### 3.3. Optimizing the coagulation–flocculation conditions

Design Expert 8.0.6 was used to calculate the response equation with a maximum HPAM removal efficiency. The optimum coagulation–flocculation conditions for maximal HPAM removal efficiency were 0.65 mg/L EPI-DMA, 924 mg/L PAFC, and pH 5.51, giving predicted HPAM and COD removal efficiencies of 94.7 and 86.4%. To verify the reliability of the fitted model, the OWPF was treated at these optimal conditions. The measured HPAM and COD removal efficiencies were 95.4 and 85.7%, respectively. This result was close to the predicted value estimated by the software, showing that the RSM optimized the coagulation–flocculation conditions well for OWPF treatment.

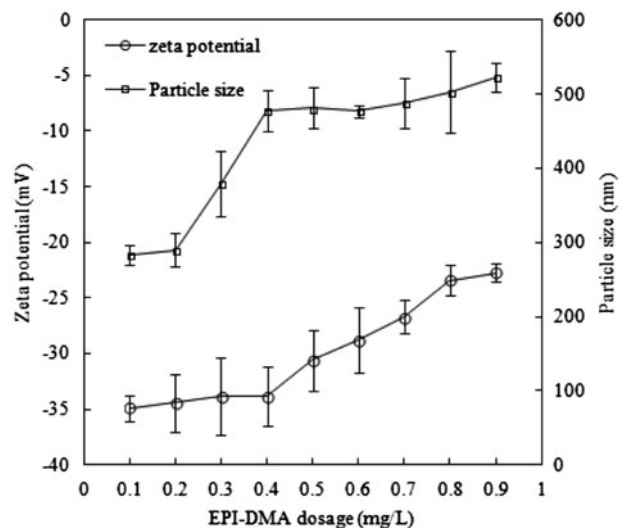


Fig. 6. Zeta potential and the particle size evolutions at the series of dosage of EPI-DMA.

### 3.4. Coagulation–flocculation mechanism

#### 3.4.1. FTIR spectra analysis

The FTIR spectra of freeze-dried samples of the OWPF, OWPF-dosed EPI-DMA, sludge, and supernatant were studied to characterize the functional groups in the samples (Fig. 5). The FTIR spectra of the samples exhibited similar peak locations, such as bands in the regions of 3,425, 1,660, and 1,600  $\text{cm}^{-1}$ , which depicted the amino group, acylamino group I (C=O stretching vibration), and acylamino group II (N–H bending vibration), respectively. The results indicated that the HPAM in the OWPF was mostly transferred to the sludge. The FTIR spectrum of the supernatant exhibited a weak acylamino group charac-

teristic peak, showing that some HPAM was left in the treated water. In the FTIR spectrum of the OWPF-dosed EPI-DMA, both the characteristic peaks of the acylamino group and EPI-DMA (1,108, 996  $\text{cm}^{-1}$ ) were clearly seen, indicating that the particles that appeared after adding the EPI-DMA were mainly a combination of HPAM and EPI-DMA. During coagulation–flocculation, the addition of positively charged quaternary ammonium from the EPI-DMA may combine with the negatively charged carboxyl group on the HPAM, destabilizing it. Thus, the main role of EPI-DMA in the coagulation–flocculation process is electrically neutral. Similar peaks at 1,140 and 1,110  $\text{cm}^{-1}$  were observed in the FTIR spectra of the treated water and sludge, indicating Fe–OH–Fe and Al–OH–Al [32].

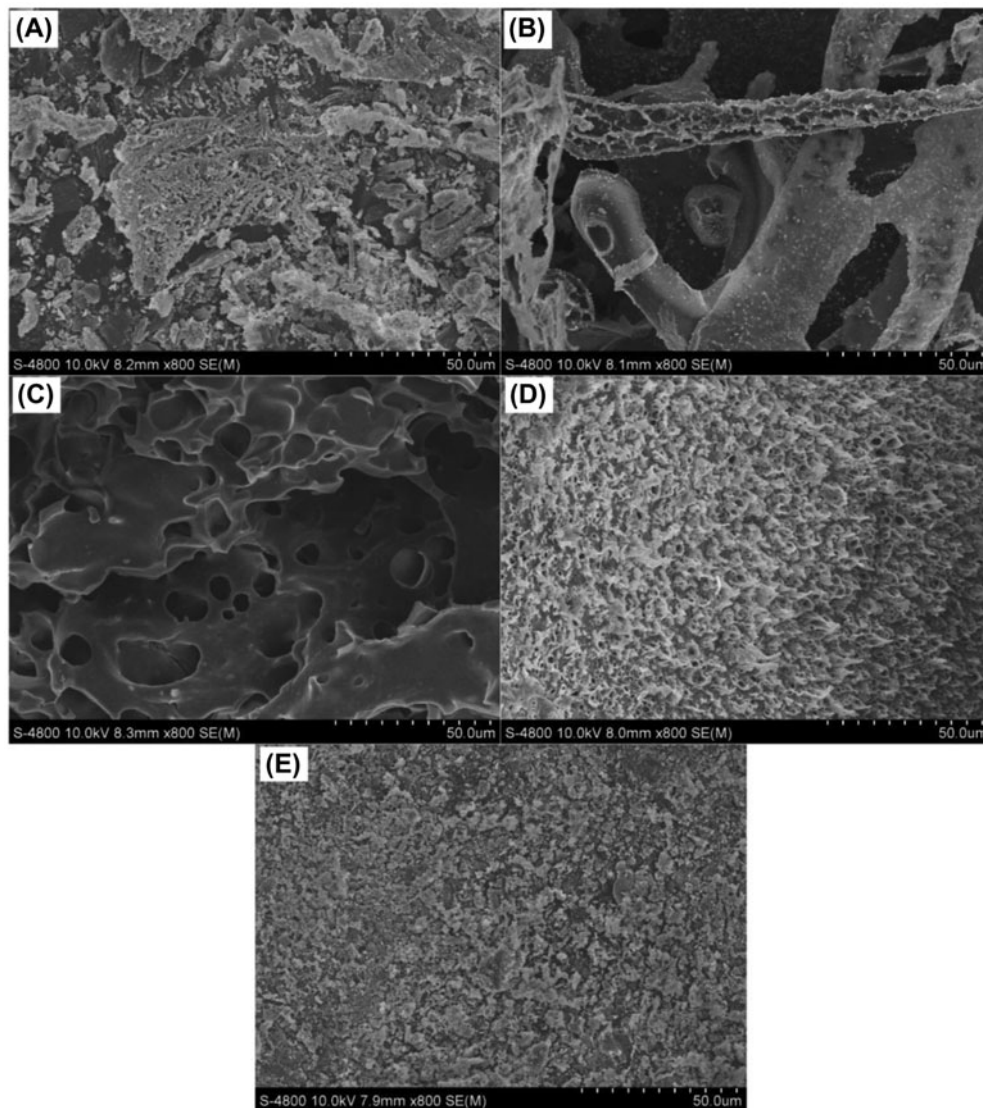


Fig. 7. SEM images of (A) OWPF, (B) raw water after dialyzing, (C) OWPF-dosed EPI-DMA, (D) sludge, and (E) supernatant.

Table 6  
EDS of OWPF, raw water after dialyzing, OWPF-dosed EPI-DMA, sludge, and supernatant

Elements (wt.%)	OWPF	Raw water after dialyzing	OWPF-dosed EPI-DMA	Sludge	Supernatant
C	20.96 ± 2.81	44.80 ± 2.82	52.53 ± 0.86	35.17 ± 0.29	10.9 ± 0.90
N	3.20 ± 0.49	11.12 ± 1.52	15.47 ± 2.20	8.61 ± 0.62	0.00 ± 0.00
O	27.84 ± 4.83	30.37 ± 2.31	29.27 ± 0.67	39.83 ± 2.16	34.23 ± 2.26
Na	26.30 ± 1.88	3.60 ± 1.22	0.64 ± 0.47	1.44 ± 0.64	27.87 ± 0.21
Al	0.00 ± 0.00	0.04 ± 0.06	1.77 ± 1.09	8.80 ± 1.31	0.00 ± 0.00
Cl	21.38 ± 3.20	6.55 ± 3.86	0.26 ± 0.27	2.98 ± 1.14	17.37 ± 3.70
Fe	0.00 ± 0.00	0.00 ± 0.00	0.00 ± 0.00	1.09 ± 0.34	0.00 ± 0.00

These FTIR spectra suggested that the transfer of the HPAM may have been due to the adsorption and sweep effect of iron and aluminum salt.

### 3.4.2. Zeta potential and particle size

Fig. 6 shows emulsion particle zeta potentials and the particle size evolution as the EPI-DMA dose changes. The experimental results in Fig. 6 show that both the zeta potential and particle size increased gradually with an increase in EPI-DMA, but followed different trends. When the flocculant dose was below 0.4 mg/L, the particle size increased obviously with the dose, whereas the zeta potential increased weakly. This result indicated that at low EPI-DMA (<0.4 mg/L), adsorption-bridging was the process implicated in the EPI-DMA flocculation mechanism. When EPI-DMA increased above 0.4 mg/L, the zeta potential increased and the particle size remained almost constant. This result suggested that the electric neutralization ability of EPI-DMA played an important role in the treatment process at high doses (>0.4 mg/L).

The EPI-DMA mechanism is therefore likely to be as follows: (1) at low doses, EPI-DMA combines with HPAM by electrostatic force, forming larger, negatively charged particles; (2) at higher flocculant doses, EPI-DMA can no longer combine with HPAM due to steric hindrance effects. The electrostatic repulsion between the EPI-DMA-HPAM combinations and the electric neutralization ability of uncombined EPI-DMA are therefore prominent.

### 3.4.3. SEM micrograph and EDS analyses

SEM micrographs are shown in Fig. 7. The HPAM in the freeze-dried sample in micrograph (B) appears as a fibrous, rod-like lump. A large amount of HPAM in the freeze-dried sample of OWPF, shown in micrograph (A), had inorganic substances adsorbed onto it. Micrograph (E) shows that the treated water contained almost no HPAM. Micrograph (C) shows that the HPAM combined with the EPI-DMA to form a dense,

porous structure. Micrograph (D) shows that PAFC generated a honeycomb-like structure with particles trapped in it, indicating the adsorption and sweeping effects of PAFC.

Table 6 shows the chemical composition of the samples. A change in carbon can be considered an indication of HPAM removal. The EDS results showed that a large amount of carbon shifted into the sludge, leaving only a little organic carbon in the supernatant. The main elements in the OWPF-dosed EPI-DMA were carbon, nitrogen, and oxygen. Only 0.55% sodium was present. It can be inferred that the  $-\text{COO}^-$  on HPAM can combine with the quaternary ammonium on EPI-DMA instead of sodium. The results were consistent with the previous analyses.

## 4. Conclusions

Coagulation–flocculation was used to treat OWPF. To maximize the removal of HPAM, the BBD, and RSM were used to optimize the EPI-DMA dose, PAFC dose, and pH. The result revealed that a maximum HPAM and COD removal of 95.4 and 85.7% could be reached using 0.65 mg/L EPI-DMA, 924 mg/L PAFC, and pH 5.51. FTIR, zeta potentials, particle size analysis, and SEM-EDS were used to study the mechanism of the coagulation–flocculation process. The results indicated that the main roles of the added EPI-DMA and PAFC in the coagulation–flocculation process were electric neutralization, adsorption, and sweep. Both the optimization and study of the mechanism have practical significance for the treatment of OWPF.

## Acknowledgment

This research was supported by the Fundamental Research Funds for the Central Universities (No. 0400219183), China Huanqiu Contracting and Engineering Corporation (No. 60058-00-0000-CA-002) and Ningbo Science and Technology Bureau (No. 2012C50038).

## References

- [1] D.K. Han, C.Z. Yang, Z.Q. Zhang, Z.H. Lou, Y.I. Chang, Recent development of enhanced oil recovery in China, *J. Pet. Sci. Eng.* 22 (1999) 181–188.
- [2] L.J. Zhang, X. Yue, F.Q. Guo, Micro-mechanisms of residual oil mobilization by viscoelastic fluids, *Pet. Sci.* 5 (2008) 56–61.
- [3] S.B. Deng, G. Yu, Z.X. Chen, D. Wu, F.J. Xia, N. Jiang, Characterization of suspended solids in produced water in Daqing oilfield, *Colloids Surf., A: Physicochem. Eng. Aspects* 332 (2009) 63–69.
- [4] X.F. Zhao, L.X. Liu, Y.C. Wang, D. Wang, H.X. Dai, H. Cai, Influences of partially hydrolyzed polyacrylamide (HPAM) residue on the flocculation behavior of oily wastewater produced from polymer flooding, *Sep. Purif. Technol.* 62 (2008) 199–204.
- [5] S.B. Deng, R.B. Bai, J.P. Chen, G. Yu, Z.P. Jiang, F.S. Zhou, Effects of alkaline/surfactant/polymer on stability of oil droplets in produced water from ASP flooding, *Colloids Surf., A: Physicochem. Eng. Aspects* 211 (2002) 275–284.
- [6] B.D. Ma, B.Y. Gao, Q.Y. Yue, Study on emulsification stability of wastewater produced by polymer flooding, *J. Pet. Sci. Eng.* 110 (2013) 27–31.
- [7] R. Yuan, Y. Li, C.X. Li, H.B. Fang, W. Wang, Study about how the metal cationic ions affect the properties of partially hydrolyzed hydrophobically modified polyacrylamide (HMHPAM) in aqueous solution, *Colloids Surf. A: Physicochem. Eng. Aspects* 434 (2013) 16–24.
- [8] H. Jiang, Q. Yu, Z. Yi, The influence of the combination of polymer and polymer-surfactant flooding on recovery, *Pet. Sci. Technol.* 29 (2011) 514–521.
- [9] P.J. Holliman, J.A. Clark, J.C. Williamson, D.L. Jones, Model and field studies of the degradation of cross-linked polyacrylamide gels used during the revegetation of slate waste, *Sci. Total Environ.* 336 (2005) 13–24.
- [10] G.R.J. Sutherland, J. Haselbach, S.D. Aust, Biodegradation of crosslinked acrylic polymers by a white-rot fungus, *Environ. Sci. Pollut. Res.* 4 (1997) 16–20.
- [11] K. Nakamiya, S. Kinoshita, Isolation of polyacrylamide-degrading bacteria, *J. Ferment. Bioeng.* 80 (1995) 418–420.
- [12] J.L. Kay-Shoemake, M.E. Watwood, R.E. Sojka, R.D. Lentz, Polyacrylamide as a substrate for microbial amidase in culture and soil, *Soil Biol. Biochem.* 30 (1998) 1647–1654.
- [13] A. Vilg -Ritter, A. Masion, T. Boulang , D. Rybacki, J.Y. Bottero, Removal of natural organic matter by coagulation-flocculation: A pyrolysis-GC-MS study, *Environ. Sci. Technol.* 33 (1999) 3027–3032.
- [14] J.G. Ottaviano, J.X. Cai, R.S. Murphy, Assessing the decontamination efficiency of a three-component flocculating system in the treatment of oilfield-produced water, *Water Res.* 52 (2014) 122–130.
- [15] O.S. Amuda, A. Alade, Coagulation/flocculation process in the treatment of abattoir wastewater, *Desalination* 196 (2006) 22–31.
- [16] B.Y. Gao, Y.Y. Jia, Y.Q. Zhang, Q. Li, Q.Y. Yue, Performance of dithiocarbamate-type flocculant in treating simulated polymer flooding produced water, *J. Environ. Sci.* 23 (2011) 37–43.
- [17] S. Verma, B. Prasad, I.M. Mishra, Pretreatment of petrochemical wastewater by coagulation and flocculation and the sludge characteristics, *J. Hazard. Mater.* 178 (2010) 1055–1064.
- [18] Y.B. Zeng, C.Z. Yang, J.D. Zhang, W.H. Pu, Feasibility investigation of oily wastewater treatment by combination of zinc and PAM in coagulation/flocculation, *J. Hazard. Mater.* 147 (2007) 991–996.
- [19] C. Desjardins, B. Koudjonou, R. Desjardins, Laboratory study of ballasted flocculation, *Water Res.* 36 (2002) 744–754.
- [20] C.Z. Hu, H.J. Liu, J.H. Qu, D.S. Wang, J. Ru, Coagulation behavior of aluminum salts in eutrophic water: Significance of Al13 species and pH control, *Environ. Sci. Technol.* 40 (2006) 325.
- [21] S.M. Miller, E.J. Fugate, V.O. Craver, J.A. Smith, J.B. Zimmerman, Toward understanding the efficacy and mechanism of *Opuntia* spp. as a natural coagulant for potential application in water treatment, *Environ. Sci. Technol.* 42 (2008) 4274–4279.
- [22] A. G rses, M. Yal ın, C. Dogar, Removal of remazol red Rb by using Al(III) as coagulant-flocculant: Effect of some variables on settling velocity, *Water Air Soil Pollut.* 146 (2003) 297–318.
- [23] K.J. Howe, A. Marwah, K.P. Chiu, S.S. Adham, Effect of coagulation on the size of MF and UF membrane foulants, *Environ. Sci. Technol.* 40 (2006) 7908–7913.
- [24] J.-P. Wang, Y.-Z. Chen, Y.Z. Wang, S.J. Yuan, H.Q. Yu, Optimization of the coagulation-flocculation process for pulp mill wastewater treatment using a combination of uniform design and response surface methodology, *Water Res.* 45 (2011) 5633–5640.
- [25] Y.F. Wang, K.F. Chen, L.H. Mo, J. Li, J. Xu, Optimization of coagulation-flocculation process for papermaking-reconstituted tobacco slice wastewater treatment using response surface methodology, *J. Ind. Eng. Chem.* 20 (2014) 391–396.
- [26] S. Mukherjee, A. Pariatamby, J.N. Sahu, B. Sen Gupta, Clarification of rubber mill wastewater by a plant based biopolymer—Comparison with common inorganic coagulants, *J. Chem. Technol. Biotechnol.* 88 (2013) 1864–1873.
- [27] J.H. Lu, L.S. Wu, Spectrophotometric determination of substrate-borne polyacrylamide, *J. Agric. Food Chem.* 50 (2002) 5038–5041.
- [28] S. Ray, J.A. Lalman, N. Biswas, Using the Box-Benken technique to statistically model phenol photocatalytic degradation by titanium dioxide nanoparticles, *Chem. Eng. J.* 150 (2009) 15–24.
- [29] R. Sen, T. Swaminathan, Response surface modeling and optimization to elucidate and analyze the effects of inoculum age and size on surfactin production, *Biochem. Eng. J.* 21 (2004) 141–148.
- [30] J.H. Choi, W.S. Shin, S.H. Lee, D.J. Joo, J.D. Lee, S.J. Choi, L.S. Park, Application of synthetic polyamine flocculants for dye wastewater treatment, *Sep. Sci. Technol.* 36 (2001) 2945–2958.
- [31] Y.F. Wang, B.Y. Gao, Q.Y. Yue, X. Zhan, X.H. Si, C.X. Li, Flocculation performance of epichlorohydrin-dimethylamine polyamine in treating dyeing wastewater, *J. Environ. Manage.* 91 (2009) 423–431.
- [32] T. Sun, C.H. Sun, G.L. Zhu, X.J. Miao, C.C. Wu, S.B. Lv, W.J. Li, Preparation and coagulation performance of poly-ferric-aluminum-silicate-sulfate from fly ash, *Desalination* 268 (2011) 270–275.